Temporal–spectral signaling of sensory information and expectations in the cerebral processing of pain

Moritz M. Nickel[a,b], Laura Tiemann[a,b], Vanessa D. Hohn[a,b], Elisabeth S. May[a,b], Cristina Gil Ávila[a,b], Falk Eippert[c], and Markus Ploner[a,b,d,1]

[a]Department of Neurology, School of Medicine, Technical University of Munich, Munich 81675, Germany; [b]Technical University of Munich Neuroimaging Center, School of Medicine, Technical University of Munich, Munich 81675, Germany; [c]Max Planck Research Group Pain Perception, Max Planck Institute for Human Cognitive and Brain Sciences, Leipzig 04103, Germany; and [d]Center for Interdisciplinary Pain Medicine, School of Medicine, Technical University of Munich, Munich 81675, Germany

The perception of pain is shaped by somatosensory information about threat. However, pain is also influenced by an individual's expectations. Such expectations can result in clinically relevant modulations and abnormalities of pain. In the brain, sensory information, expectations (predictions), and discrepancies thereof (prediction errors) are signaled by an extended network of brain areas which generate evoked potentials and oscillatory responses at different latencies and frequencies. However, a comprehensive picture of how evoked and oscillatory brain responses signal sensory information, predictions, and prediction errors in the processing of pain is lacking so far. Here, we therefore applied brief painful stimuli to 48 healthy human participants and independently modulated sensory information (stimulus intensity) and expectations of pain intensity while measuring brain activity using electroencephalography (EEG). Pain ratings confirmed that pain intensity was shaped by both sensory information and expectations. In contrast, Bayesian analyses revealed that stimulus-induced EEG responses at different latencies (the N1, N2, and P2 components) and frequencies (alpha, beta, and gamma oscillations) were shaped by sensory information but not by expectations. Expectations, however, shaped alpha and beta oscillations before the painful stimuli. These findings indicate that commonly analyzed EEG responses to painful stimuli are more involved in signaling sensory information than in signaling expectations or mismatches of sensory information and expectations. Moreover, they indicate that the effects of expectations on pain are served by brain mechanisms which differ from those conveying effects of sensory information on pain.

pain | brain | electroencephalography | oscillations | predictive coding

T he perception of pain emerges from the integration of sensory information about threat and contextual factors such as an individual's expectations (1–3). For instance, expectations of pain relief during placebo manipulations can yield substantial and clinically highly relevant decreases of pain (4–6). Moreover, expectations cannot only alleviate pain but also significantly influence the development (7) and prognosis of chronic pain (8, 9). Thus, understanding how the brain translates sensory information and expectations into pain promises important insights into the neural mechanisms of pain in health and disease.

In the brain, pain is associated with the activation of an extended network of brain areas (10, 11) which yields electrophysiological responses at different latencies and frequencies (12). These responses comprise evoked potentials including the early N1 and later N2 and P2 components (13, 14) as well as oscillatory responses at alpha (8 to 13 Hz), beta (13 to 30 Hz), and gamma (40 to 100 Hz) frequencies (15). Electroencephalography (EEG) and magnetoencephalography (MEG) studies have provided important insights into the functional significance of these responses. The early N1 response has been particularly related to objective sensory information, while the later N2 and P2 components (16, 17) as well as gamma oscillations (18, 19) are more closely related to subjective pain perception. However,

results on how expectations shape the different responses are inconsistent (20–29). Thus, a comprehensive assessment of how different evoked and oscillatory brain responses signal sensory information, expectations, and pain is lacking so far.

The predictive coding framework of brain function (30, 31) is a general theory used to describe the encoding and integration of sensory information and expectations (32). The framework proposes that the brain continuously generates predictions about the environment. These predictions are compared against sensory evidence, and discrepancies produce prediction errors (PEs) that serve to optimize future predictions. In this way, the brain efficiently allocates its limited resources to events that are behaviorally relevant and useful for updating predictions [i.e., learning processes (33)]. It has been suggested that predictive coding processes are implemented by evoked potentials at different latencies (34) and neuronal oscillations at different frequencies (35, 36). In particular, it has been shown that already the earliest evoked potential components are shaped by predictions (37, 38), whereas later responses have been related to PEs (39). Moreover, alpha and beta oscillations have been implicated in the signaling of predictions, whereas gamma oscillations have been proposed to signal PEs (35, 36, 40–42).

Significance

Pain is not only shaped by sensory information but also by an individual's expectations. Here, we investigated how commonly analyzed electroencephalography (EEG) responses to pain signal sensory information, expectations, and discrepancies thereof (prediction errors) in the processing of pain. Bayesian analysis confirmed that pain perception was shaped by objective sensory information and expectations. In contrast, EEG responses at different latencies (including the N1, N2, and P2 components) and frequencies (including alpha, beta, and gamma oscillations) were shaped by sensory information but not by expectations. Thus, EEG responses to pain are more involved in signaling sensory information than in signaling expectations or prediction errors. Expectation effects are obviously mediated by other brain mechanisms than the effects of sensory information on pain.
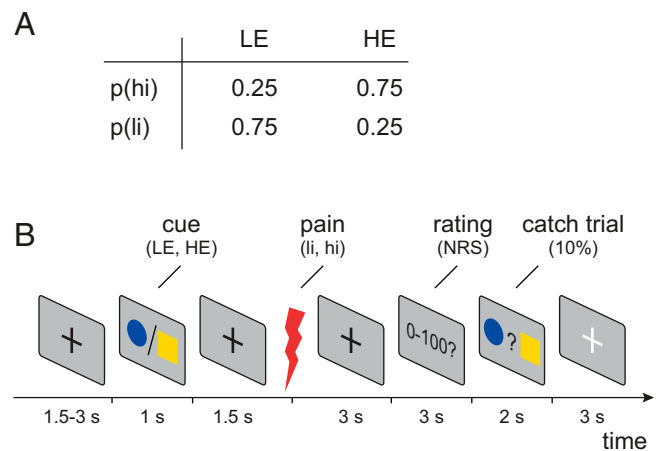
Considering the preeminent role of the integration of sensory information and expectations in the processing of pain, an application of predictive coding frameworks to pain is obvious (15, 43–46). This is even more appealing as abnormally precise predictions and/or abnormal updating of predictions might figure prominently in the pathology of chronic pain (47–49). Consequently, recent functional magnetic resonance imaging (fMRI) studies have applied predictive coding frameworks to the processing of pain (50, 51). The results revealed a spatial dissociation of the encoding of stimulus intensity, predictions, and PEs in the processing of pain. Most recently, a first EEG study applied a predictive coding framework to oscillatory responses to noxious stimuli (52). The findings indicated that alpha-to-beta and gamma oscillations signal expectations and PEs in the processing of pain, respectively. However, a model which comprehensively describes how evoked potentials at different latencies—which are the electrophysiological gold standard for assessing the cerebral processing of pain—and oscillations at different frequencies signal sensory information, expectations, and PEs in the processing of pain is lacking so far.

To systematically investigate whether and how evoked and oscillatory EEG responses to pain signal stimulus intensity, expectations, and PEs, we applied brief painful stimuli to healthy human participants and independently modulated sensory information and expectations. We hypothesized that alpha/beta and gamma oscillations signal predictions and PEs, respectively. We further expected that already the earliest evoked responses to noxious stimuli are shaped by predictions, whereas later responses are also shaped by PEs. To test these hypotheses, we performed Bayesian ANOVAs and model comparisons on pain ratings and EEG responses. Pain ratings confirmed that pain intensity was shaped by both sensory information and expectations. In contrast, EEG responses at different latencies (N1, N2, and P2 components) and frequencies (alpha, beta, and gamma oscillations) were shaped by sensory information but not by expectations. Together, these findings reveal that commonly analyzed EEG responses to painful stimuli are more sensitive to sensory information than to expectations or PEs. Moreover, they indicate that expectations effects on pain are served by other brain mechanisms than sensory effects on pain.

Results

To investigate how EEG responses to brief painful stimuli signal stimulus intensity, expectations, and PEs in the processing of pain, we employed a probabilistic cueing paradigm in 48 healthy human participants. We applied brief painful heat stimuli to the left hand and independently modulated stimulus intensity and expectations in a 2 × 2 factorial design. To modulate stimulus intensity, we applied painful stimuli of two different levels (high intensity [hi] and low intensity [li]). To modulate expectations, the painful stimuli were preceded by one out of two visual cues. The high-expectation (HE) cue was followed by a hi stimulus in 75% of the trials and by a li stimulus in 25% of the trials. Vice versa, the low-expectation (LE) cue was followed by a hi stimulus in 25% of the trials and by a li stimulus in 75% of the trials. The experiment thus comprised four trial types (Fig. 1A): high intensity, high expectation (hiHE); high intensity, low expectation (hiLE); low intensity, high expectation (liHE); and low intensity, low expectation (liLE). In each trial, the participants were asked to provide a rating of the perceived pain intensity on a numerical rating scale ranging from 0 (no pain) to 100 (maximum tolerable pain). In addition, skin conductance responses (SCRs) were recorded. Fig. 1B shows the sequence of a single trial.

During the experiment, we recorded EEG and assessed the most consistently observed EEG responses to painful stimuli (12). Evoked EEG responses included the N1, N2, and P2 components. Oscillatory responses included stimulus-induced
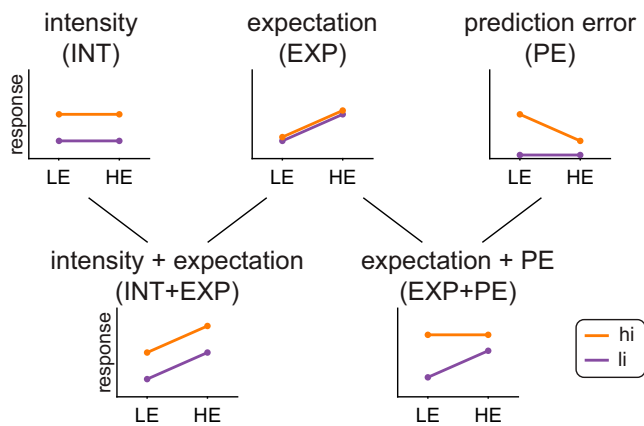

Fig. 1. Experimental design. (A) Probabilities of high- and low-intensity stimuli (p(hi) and p(li), respectively) in HE and LE trials. (B) Each trial started with a central fixation cross with a varying duration of 1.5 to 3 s followed by either a blue dot or yellow square as visual cue. Cues were presented for 1 s and indicated the probability of a subsequent high-intensity painful stimulus (0.75 for HE cue or 0.25 for LE cue). The association between the blue dot/yellow square and high-intensity (hi)/low-intensity (li) painful stimuli was balanced across participants. At 1.5 s after the offset of the cue presentation, a painful heat stimulus was applied (3.5 J for high-intensity and 3.0 J for low-intensity stimuli). At 3 s after the onset of the painful heat stimulus, participants were asked to verbally rate the perceived pain intensity on a numerical rating scale (NRS) ranging from 0 (no pain) to 100 (maximum tolerable pain). In 10% of the trials, a match-to-sample task ensured attention to the cues. In these catch trials, participants were prompted to select the cue that had been displayed during the current trial by a button press. Trials were separated by a break of 3 s, during which a white fixation cross was presented.

changes of alpha, beta, and gamma oscillations. In addition, we quantified brain activity before the painful stimulus, including the stimulus preceding negativity [SPN (29)] and oscillatory activity at alpha and beta frequencies.

Building upon previous investigations (50, 53), we made specific predictions how EEG responses signaling stimulus intensity, expectations, PEs, or combinations thereof are modulated across the four trial types (Fig. 2).

To formally test these predictions, we pursued two complementary approaches (50, 53). First, we performed repeated measures ANOVAs (rmANOVAs) with the independent variables stimulus intensity and expectation. In these rmANOVAs, responses signaling stimulus intensity and expectations would manifest as main effects, whereas responses signaling PEs would manifest as interactions. To quantify effects and to facilitate interpretation of negative findings, we primarily performed Bayesian rmANOVAs (54). In Bayesian rmANOVAs, the Bayes factor (BF) is the ratio between the likelihood of the data given the effect of interest and the likelihood of the data without the effect of interest. BF > 3 and BF > 10 indicate moderate and strong evidence in favor of the effect of interest, whereas BF < 0.33 and BF < 0.1 indicate moderate and strong evidence against the effect of interest, respectively (54). Complementing Bayesian inference, we also performed traditional frequentist rmANOVAs. Detailed results of both Bayesian and frequentist rmANOVAs are provided in *SI Appendix*, Tables S1–S3. Second, we employed Bayesian model comparisons based on single-trial data to formally test which combination of stimulus intensity, expectations, and PEs best explained the observed EEG responses. Building upon previous studies (50, 53), we specifically compared models where stimulus intensity only (INT model), stimulus intensity and expectations (INT+EXP), and

Fig. 2. Predicted response patterns for responses signaling stimulus intensity (INT model), expectations (EXP model), prediction errors (PE model), or combinations thereof (INT+EXP model, EXP+PE model).

expectations and PE (EXP+PE) shaped the respective responses. In line with a previous study (50), the PE was defined as aversive PE, meaning that a PE occurs only if the stimulus is more painful than expected. This model has been shown to outperform models with absolute and signed PE formulations (50) (see *SI Appendix,* Fig. S2 for Bayesian model comparisons using absolute and signed PE formulations).

The Effects of Stimulus Intensity, Expectations, and PEs on Pain Ratings and SCR. Before analyzing EEG responses, we investigated the effects of stimulus intensity, expectations, and PEs on pain intensity ratings. We therefore calculated rmANOVAs with the independent variables stimulus intensity and expectation. Results are shown in Fig. 3 and *SI Appendix,* Table S1. BFs indicated strong evidence for main effects of stimulus intensity (BF = 1.6×10^{26}) and expectations (BF = 1.2×10^{4}). Specifically, pain intensity was higher for hi than for li stimuli and higher for HE than for LE trials. Bayesian rmANOVA showed weak evidence against an interaction of stimulus intensity and expectation (BF = 0.36). To further investigate the relationship between stimulus intensity, expectations, PEs, and pain ratings, we tested INT, INT+EXP, and EXP+PE models against each other. The comparisons showed strong evidence that the INT+EXP model explained the data better than the INT (BF = 7.8×10^{20}) or the EXP+PE (BF = 2.8×10^{-45}) model. Thus, we found that stimulus intensity and expectations, but not PEs shaped pain ratings.

We next investigated how stimulus intensity, expectations and PEs shaped SCR. The rmANOVA for the SCR showed strong evidence for a main effect of stimulus intensity (BF = 3.2×10^{12}), i.e., the amplitude of SCRs was higher in hi than in li trials (*SI Appendix,* Fig. S1 and Table S1). However, we found inconclusive evidence regarding a main effect of expectation (BF = 0.68) and weak evidence against an interaction of stimulus intensity and expectation (BF = 0.24) on SCR. Bayesian model comparisons of single-trial SCRs showed evidence that the INT model explained the SCR just as well as the INT+EXP model (BF = 1.0) and better than the EXP+PE (BF = 1.4×10^{-4}) model (Fig. 3).
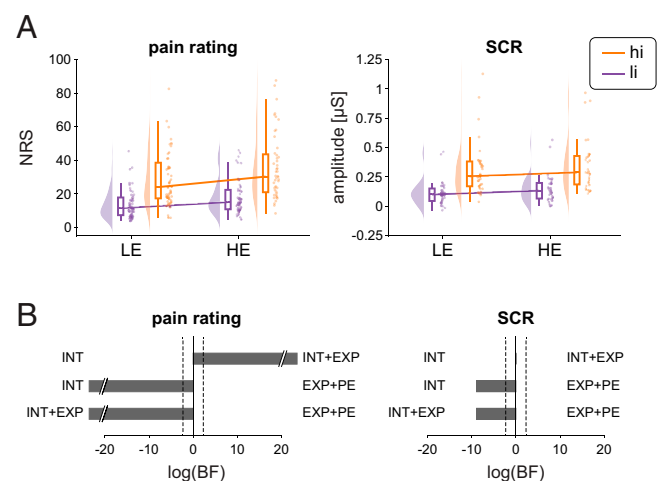
Taken together, we found strong effects of stimulus intensity on pain intensity ratings and SCRs. Moreover, we found a strong effect of expectations on pain intensity but only inconclusive evidence for an effect of expectations on SCRs. Furthermore, we did not observe an interaction between stimulus intensity and expectation in shaping pain ratings and SCRs.

The Effects of Stimulus Intensity, Expectations, and PEs on EEG Responses to Noxious Stimuli. To investigate the effects of stimulus intensity, expectations, and PEs on EEG responses, we calculated rmANOVAs as done for pain intensity ratings and SCR. Bayesian rmANOVAs showed strong evidence for a main effect of stimulus intensity on all EEG responses (BF > 1.2×10^{3}). N1, N2, and P2 responses (Fig. 4 and *SI Appendix,* Table S2) as well as poststimulus gamma oscillations and alpha and beta suppressions (Fig. 5 and *SI Appendix,* Table S3) were stronger in the hi than in the li conditions. Further analyses with baseline correction of EEG responses yielded similar results (*SI Appendix,* Table S4).
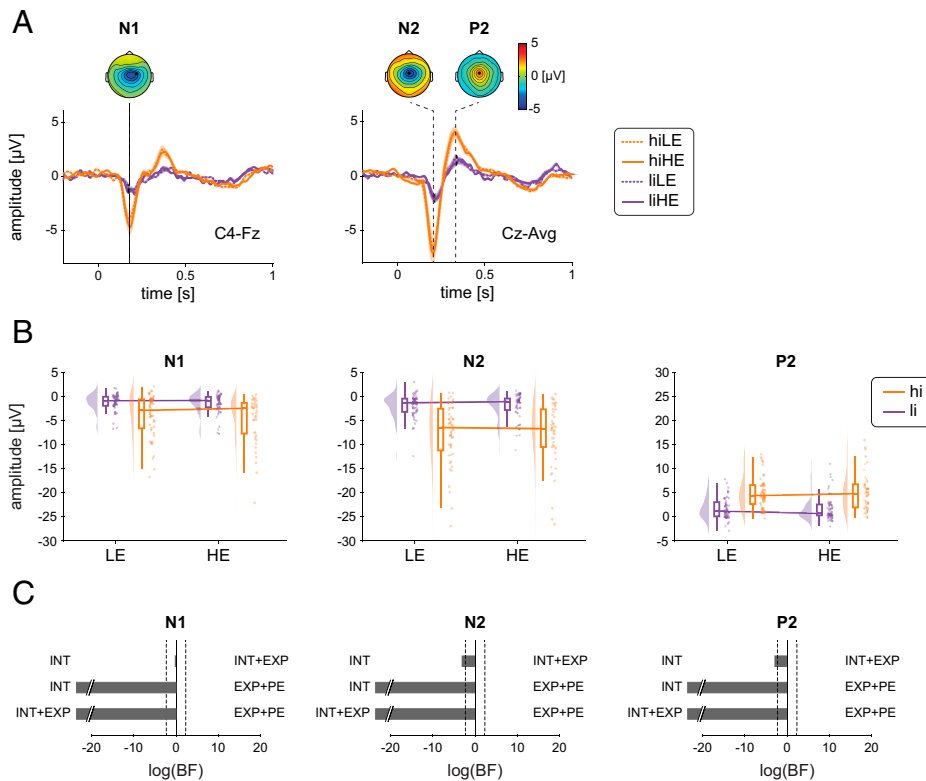
In contrast, we found moderate evidence against an expectation effect on all EEG responses (all BF < 0.22) apart from the N1, where evidence was inconclusive (BF = 0.39). In addition, we found moderate evidence against an interaction of stimulus intensity and expectation for all EEG responses (all BF < 0.26). We, thus, observed that the most consistently observed evoked and oscillatory EEG responses to noxious stimuli were shaped by stimulus intensity but not by expectations or PEs.

To test for effects on brain activity other than the predefined EEG responses, ANOVAs and cluster-based permutation tests were performed across the poststimulus time period from 0 to 1 s, all frequencies, and all channels which corroborated the results at alpha, beta, and gamma frequencies (*SI Appendix,* Fig. S3). Accordingly, model comparisons for N1, N2, and P2, alpha, beta, and gamma responses yielded stronger evidence for the INT model than for the INT+EXP (BF < 0.10) and EXP+PE (BF < 0.012) models, except for the N1, which showed inconclusive evidence regarding the comparison of the INT and the INT+EXP models (BF = 0.84). Thus, poststimulus EEG responses were consistently modulated by stimulus intensity but not by expectations.

Having found no expectation effects on EEG responses, we further asked whether the expectation effect on pain ratings

Fig. 3. Effects of stimulus intensity, expectations, and PEs on pain ratings and SCR. (*A*) Raincloud plots (55) of pain ratings and SCRs in hiLE, hiHE, liLE, and liHE conditions. The clouds display the probability density function of the individual means, indicated by dots. Boxplots depict the sample median as well as first (Q1) and third quartiles (Q3). Whiskers extend from Q1 to the smallest value within Q1 − 1.5 × interquartile range (IQR) and from Q3 to the largest values within Q3 + 1.5 × IQR. (*B*) Bayesian model comparisons between stimulus intensity (INT) and stimulus intensity + expectations (INT+EXP) models, stimulus intensity (INT) and expectations + PE (EXP+PE) models, and stimulus intensity + expectations (INT+EXP), and expectations + PE (EXP+PE) models. The bars depict the natural logarithm of the BFs. The discontinuous bars indicate log(BF) > 20 or log(BF) < −20. The dotted lines indicate the bounds of strong evidence (log(BF = 0.1) and log(BF = 10)) (54).

Nickel et al.
Temporal–spectral signaling of sensory information and expectations in the cerebral processing of pain

PNAS | 3 of 10
https://doi.org/10.1073/pnas.2116616119

Fig. 4. Effects of stimulus intensity, expectations, and PEs on evoked EEG responses to noxious stimuli. (*A*) Grand averages of evoked EEG responses. Orange and violet shadings indicate the SEM. Topographies are based on the average of all four conditions at peak latencies. (*B*) Raincloud plots (55) of N1, N2, and P2 amplitudes in hiLE, hiHE, liLE, and liHE conditions. The clouds display the probability density function of the individual means indicated by dots. Boxplots depict the sample median as well as first (Q1) and third quartiles (Q3). Whiskers extend from Q1 to the smallest value within $Q1 - 1.5 \times$ interquartile range (IQR) and from Q3 to the largest values within $Q3 + 1.5 \times$ IQR. (*C*) Bayesian model comparisons between stimulus intensity (INT) and stimulus intensity + expectations (INT+EXP) models, stimulus intensity (INT) and expectations + PE (EXP+PE) models, and stimulus intensity + expectations (INT+EXP), and expectations + PE (EXP+PE) models. The bars depict the natural logarithm of the BFs. The discontinuous bars indicate log(BF) > 20 or log(BF) < −20. The dotted lines indicate the bounds of strong evidence (log(BF = 0.1) and log(BF = 10)) (54).

can be explained by a pattern of the different EEG responses rather than each response in isolation. We therefore performed a multiple regression analysis to test whether difference values (HE − LE) of N1, N2, P2, and alpha, beta, and gamma responses together capture the expectation effect on pain ratings. However, the multiple regression model did not explain a significant amount of variance in the data ($F_{(6, 44)} = 0.66$; $P = 0.68$; $R^2 = 0.094$).
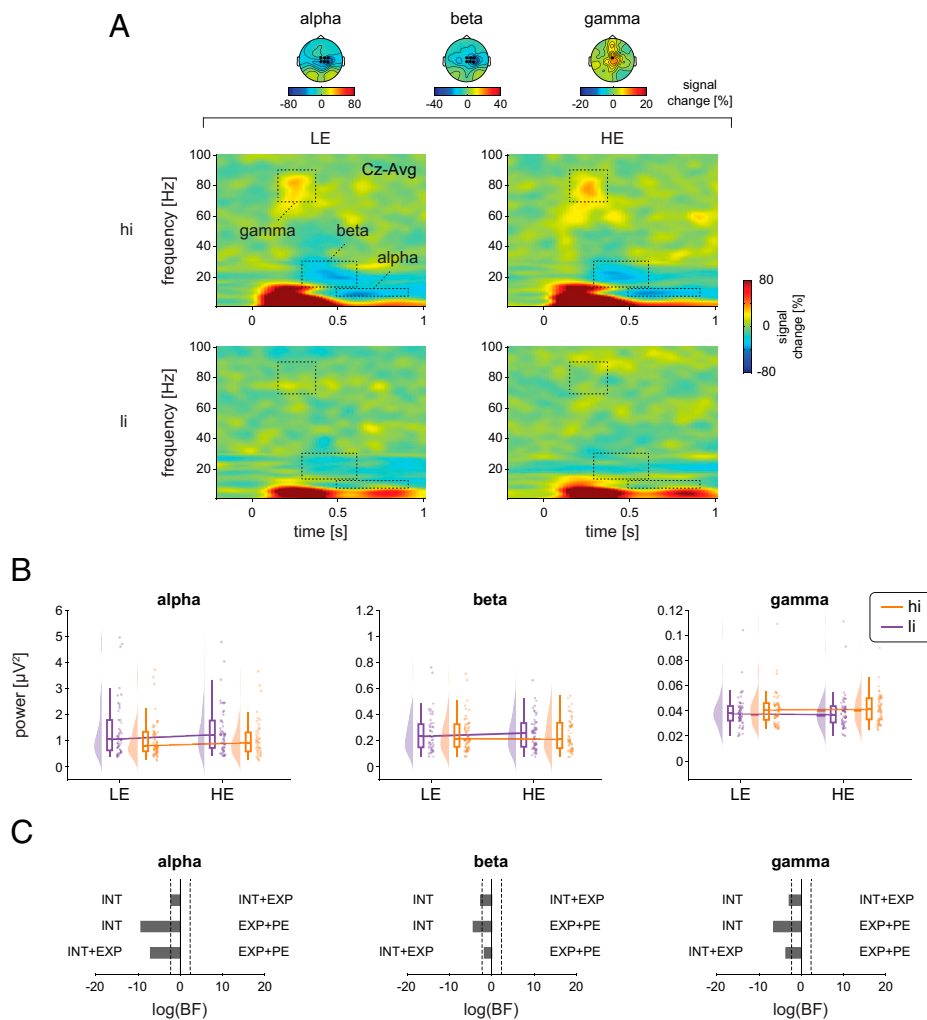
In summary, results from rmANOVAs and model comparisons convergingly showed that stimulus intensity shapes all EEG responses. In contrast, we found evidence against an effect of expectations and/or PEs on EEG responses. Moreover, expectation effects on pain ratings were neither captured by any single EEG response nor by their combination.

The Effects of Expectations on EEG Activity before the Noxious Stimuli. Lastly, expectations might not only influence poststimulus responses to a painful stimulus but also shape brain activity in anticipation of the painful stimulus. We utilized the high temporal resolution of EEG to disentangle these effects. Specifically, we analyzed the SPN reflected by the average amplitude at Cz during 500 ms directly preceding the laser stimulus. In addition, we analyzed oscillatory brain activity during two prestimulus phases [i.e., during cue presentation and between cue presentation and painful stimulus (Fig. 6*A* and *SI Appendix*, Table S5)]. Bayesian-dependent samples Student's *t* tests showed evidence against an expectation effect on the SPN (BF = 0.17). In contrast, expectations significantly influenced oscillatory brain activity at alpha and beta frequencies (Fig. 6*B*

and *SI Appendix*, Table S5). In particular, the cue-induced decrease in alpha oscillations was stronger for HE trials than for LE trials (BF = 98.8 for the cue presentation phase, BF 2.0 for the phase between cue presentation and painful stimuli). In addition, the cue-induced decrease in beta oscillations was stronger for HE than for LE trials (BF = 8.5 for the phase between cue presentation and pain stimulus). These results were corroborated by cluster-based permutation tests, which were performed less restrictively across time, frequencies, and all channels (*SI Appendix*, Fig. S2). The cluster-based permutation tests were performed separately for the period of cue presentation and for the period closely preceding the painful stimulus. We thus found that expectations shaped neuronal oscillations at alpha and beta frequencies before the painful stimulus.

Discussion

In the present study, we observed that sensory information significantly shaped the perception of pain and EEG responses commonly associated with pain. Expectations, in contrast, modulated the perception of pain but not associated EEG responses. Bayesian hypothesis testing confirmed that the observed lack of expectation effects on EEG responses can indeed be interpreted as an absence of effects. These findings indicate that commonly analyzed EEG responses to painful stimuli are more involved in signaling sensory information than in signaling expectations or mismatches of sensory information and expectations. Moreover, they indicate that the effects of
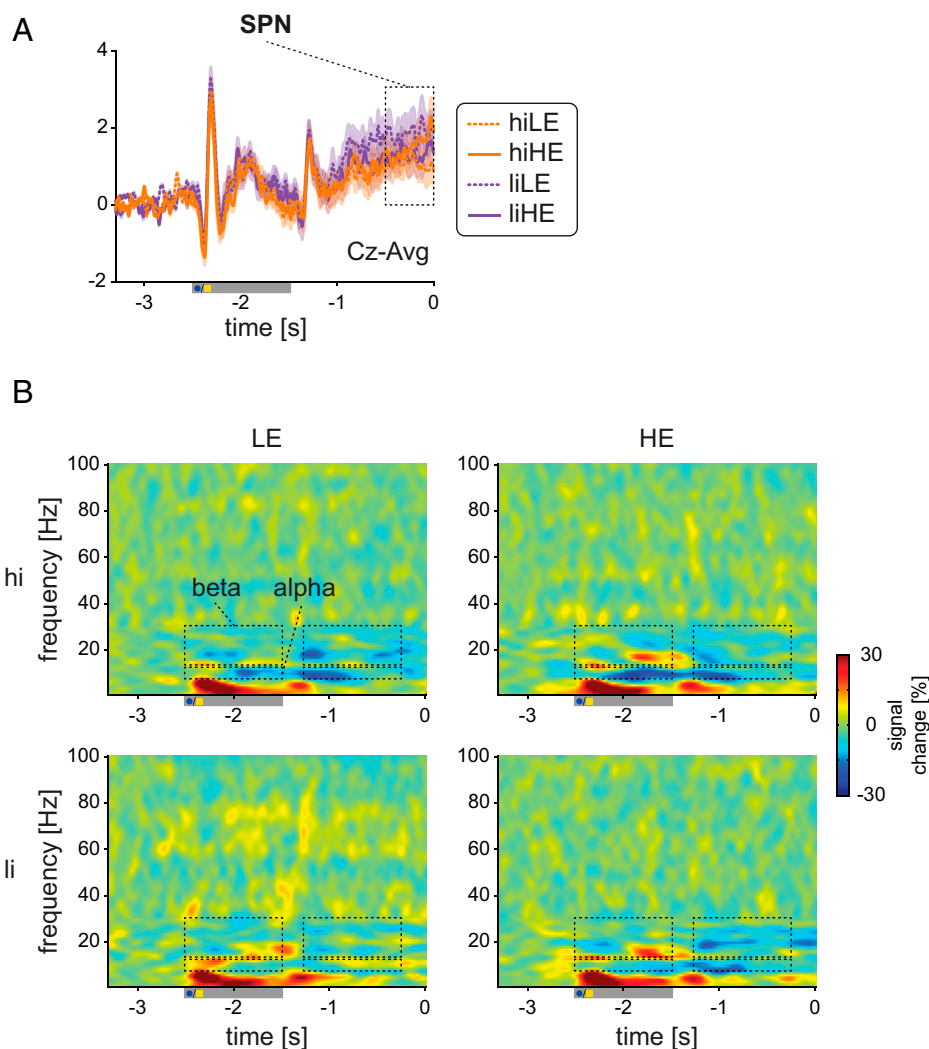
Fig. 5. Effects of stimulus intensity, expectations, and PEs on oscillatory EEG responses to noxious stimuli. (*A*) Grand averages of time-frequency representations (TFRs) are depicted as relative change to the baseline preceding the cue presentation (−3.3 to −2.8 s). For visualization, TFRs at Cz are presented. Statistical analysis was performed on absolute power values without baseline correction averaged across ROIs as indicated by the dotted boxes and marked electrodes. Topographies display the average of ROIs across all four conditions. (*B*) Raincloud plots (55) of alpha, beta, and gamma power in hiLE, hiHE, liLE, and liHE conditions. The clouds display the probability density function of the individual means indicated by dots. Boxplots depict the sample median as well as first (Q1) and third quartiles (Q3). Whiskers extend from Q1 to the smallest value within Q1 − 1.5 × interquartile range (IQR) and from Q3 to the largest values within Q3 + 1.5 × IQR. (*C*) Bayesian model comparisons between stimulus intensity (INT) and stimulus intensity + expectations (INT+EXP) models, stimulus intensity (INT) and expectations + PE (EXP+PE) models, and stimulus intensity + expectations (INT+EXP), and expectations + PE (EXP+PE) models. The bars depict the natural logarithm of the BFs. The discontinuous bars indicate log(BF) > 20 or log(BF) < −20. Dotted lines indicate the bounds of strong evidence (log(BF = 0.1) and log(BF = 10)) (54).

expectation on pain are served by different brain mechanisms than those conveying effects of sensory information on pain and are not well captured by commonly analyzed EEG responses to noxious stimuli. We will discuss the implications of these findings for understanding the functional significance of EEG responses to pain, particularly in the context of predictive coding frameworks of brain function, and for understanding how the brain mediates expectation effects on pain.

The Functional Significance of Pain-Associated EEG Responses. Our observation that stimulus intensity shapes EEG responses to noxious stimuli is in accordance with previous studies which nearly uniformly showed such effects. Expectation effects, on the other hand, were limited to pain ratings and not found for EEG responses in the present study. At first glance, this contrasts with previous studies, which have shown that expectations significantly modulate EEG responses (20–27). However, expectation effects in those studies were weaker and less

consistent than stimulus intensity effects. Moreover, limited statistical power (56) and publication bias (57) might have resulted in an overestimation of expectation effects across the literature. Thus although expectations can, in principle, shape EEG responses, the present findings indicate that these responses are more sensitive to stimulus intensity effects than to expectations. Whether this fundamental difference generalizes from expectations to other contextual modulations of pain remains to be determined. Moreover, whether these observations are specific for EEG responses to pain or generalize to EEG responses to sensory events from other modalities remains unclear.

Pain-Associated EEG Responses in a Predictive Coding Model of Brain Function. As the interaction of sensory evidence and predictions crucially shapes the perception of pain, predictive coding frameworks of brain function have been increasingly applied to the processing of pain (15, 43–46). Based on these

Nickel et al.
Temporal–spectral signaling of sensory information and expectations in the cerebral processing of pain

PNAS | 5 of 10
https://doi.org/10.1073/pnas.2116616119

Fig. 6. The effects of expectations on EEG activity before the noxious stimuli. (*A*) Grand averages of time-domain signals at Cz are depicted, which preceded the laser stimulus. Orange and violet shadings denote the SEM. The amplitude of the SPN was determined by averaging the signal at Cz between −0.5 and 0 as indicated by the dotted box. Painful stimulus onset occurs at t = 0. The gray bar *Below* the x-axis indicates the time period of cue presentation. (*B*) Grand averages of the time-frequency representation are depicted as relative change to the baseline preceding the cue presentation (−3.3 to −2.8 s). The dotted boxes represent the two different time windows considered at the alpha and beta frequencies. Painful stimulus onset occurs at t = 0. The gray bar *Below* the x-axis indicates the time period of cue presentation. The data were averaged across channels Cz, C2, C4, CPz, CP2, and CP4 and across time and frequency points as indicated by the dotted boxes. Statistical analysis was performed on absolute power values without baseline correction.

considerations, recent functional imaging studies have started to investigate how the brain encodes sensory information, predictions, and PEs in the processing of pain (50, 51). The results have revealed a spatial dissociation between brain areas encoding stimulus intensity, predictions, and PEs. More precisely, a dissociation was found in the insular cortex where posterior parts signaled sensory information, whereas anterior parts additionally signaled predictions and PEs. The present study was inspired by these investigations and adapted their paradigm for EEG. We particularly aimed to assess how evoked and oscillatory brain responses at different latencies and frequencies encode sensory information, expectations, and PEs. Based on previous anatomical and physiological evidence (35, 36, 41, 42), we specifically hypothesized that alpha/beta and gamma oscillations signal predictions and PEs, respectively. We further expected that already the earliest laser-evoked responses are shaped by predictions (37, 38), whereas later responses are also shaped by PEs (39).

Our observed prestimulus effects support the idea that alpha/beta oscillations are indeed involved in signaling predictions also in the context of pain. However, Bayesian hypothesis testing of poststimulus effects provided evidence against the hypothesis that predictions and PEs shape evoked and oscillatory responses to noxious stimuli. This contrasts with the results of a recent EEG study (52), which showed that poststimulus alpha/beta oscillations and gamma oscillations were shaped by predictions and PEs, respectively. This difference between the previous and the present study might be due to different durations of the employed noxious stimulation models. The previous study used contact-heat stimuli of a few-seconds duration, whereas the present study used radiant-heat laser stimuli of a few-milliseconds duration. Laser stimuli are a standard tool for research on the brain mechanisms of pain and for the clinical assessment of nociceptive pathways (58). They yield a highly synchronized activation of nociceptive afferents, resulting in a short and clear-cut pain sensation. These stimuli therefore offer

the opportunity to not only detect non–phase-locked oscillatory responses but to also to record phase-locked evoked responses and to determine their role in signaling sensory information, expectations, and PEs as previously done in other modalities (59, 60). However, predictive coding concepts propose that the precision of sensory information and predictions crucially determines their weight in further processing (43). Thus the brief laser stimuli of the present study might yield sensory information with a high precision and weight, which in turn might result in a relative down weighting of predictions. Hence, for very brief and clear-cut stimuli, the influence of sensory information might outweigh the influence of predictions and PEs on EEG responses.

In the present study, we performed direct Bayesian model comparisons to assess the role of EEG responses in the signaling of sensory evidence, expectations, and PEs in the processing of pain. While our results reveal that evoked and oscillatory EEG responses—which are commonly used to assess brain processes related to pain for research and clinical practice—are more involved in signaling sensory evidence than expectations or PEs, it is important to note that these findings do neither argue in favor of nor against predictive coding models of brain function. Our findings should thus not discourage the application of predictive coding frameworks to the processing of pain but rather encourage the search for brain features—other than the commonly analyzed EEG responses—that signal predictions and PEs in the processing of pain. Such future approaches might build upon recent predictive coding models for nociceptive processing in animals (61) and for the perception of stimuli from other modalities in humans (40).

Brain Mechanisms of Expectation Effects on Pain. Our observation of expectation effects on the perception of painful stimuli without effects on associated EEG responses support that neither evoked nor oscillatory EEG responses to noxious stimuli represent a reliable correlate of pain (62). This dissociation might also be relevant for the search for brain-based biomarkers of pain (63). Instead, our findings indicate that EEG responses rather represent a correlate of sensory processing, which is not always sensitive to contextual modulations. Thus, other processes not captured by commonly analyzed EEG responses to noxious stimuli likely contribute to contextual modulations of pain. These processes might include cognitive evaluation, pain affect, decision making, and reward processing. Such higher-level processes might be less strictly time locked to noxious stimuli and might therefore not be captured by commonly analyzed EEG responses. Furthermore, these processes might take place in deeper brain areas such as the striatum, medial temporal lobe areas, and the brainstem, which are involved in expectation effects on pain (64–67) but are not well captured by EEG. Moreover, expectation effects might not manifest in evoked potentials and/or oscillatory responses on the sensor level, as these are a mixture of neural responses from different brain areas but might only manifest in certain brain areas. Thus source space analyses—which can help to disentangle mixtures of neural responses from different brain areas—might be more sensitive to expectation effects than sensor space analysis. Moreover, such source space analyses also allow for analyzing connectivity between sources. Considering the high complexity of the pain experience and its cerebral substrates, such connectivity analyses are particularly promising. However, source space analyses of EEG signals are inherently ambiguous, and common EEG approaches to the cerebral processing of pain therefore rely on sensor space as done in the current study.

In this way, the current EEG findings complement fMRI studies showing that the influence of contextual factors including expectations and placebo effects on pain are mediated by spatial patterns other than those capturing sensory processing

(68–70). This is also in accordance with previous fMRI studies on predictive coding in the processing of pain, which showed that the nociceptive sensitive neurologic pain signature was mostly shaped by stimulus intensity rather than expectations (50, 51). Moreover, expectation effects on pain are likely not homogenous. For instance, it has been shown that expectation effects induced by social information and associated learning (71) as well as positive and negative expectation effects (66) differ fundamentally.

Conclusions. The present results indicate that commonly analyzed EEG responses to noxious stimuli are more sensitive to sensory processes than to expectations or mismatches between sensory processes and expectations. This finding provides insights into the functional significance of the complex spatial–temporal–spectral patterns of brain activity associated with pain. Moreover, our observations might motivate and guide further investigations on how the brain signals sensory information, predictions, and PEs in the processing of pain. Understanding these processes might also have implications for understanding the brain mechanisms of chronic pain, which have been related to abnormally precise predictions (47–49).

Materials and Methods

Participants. This study was performed in healthy human participants who were recruited through advertisements on an online platform of the Technical University of Munich. Prior to any experimental procedures, all participants gave written informed consent. The study protocol was approved by the Ethics Committee of the Medical Faculty of the Technical University of Munich and preregistered at ClinicalTrials.gov (NCT04296968). The study was conducted in accordance with the latest version of the Declaration of Helsinki and followed recent guidelines for the analysis and sharing of EEG data (72).

Inclusion criteria were age above 18 y and right-handedness. Exclusion criteria were pregnancy, neurological or psychiatric diseases, severe internal diseases including diabetes, skin diseases, current or recurrent pain, regular intake of medication (aside from contraception and thyroidal medication), previous surgeries at the head or spine, metal or electronic implants, and any previous side effects associated with thermal stimulation.

A priori sample size calculations using G*Power (73) determined a sample size of 36 participants for a rmANOVA design with one group and four measurements (see *Procedure* for conditions), a power of 0.95, an alpha of 0.05, and medium effect sizes of f = 0.25. This corresponds to an η^2 (proportion variance explained) of 0.06 (74). Overall, 58 healthy human participants (29 females, age: 24.0 ± 4.3 y [mean ± SD]) were recruited. Nine participants were excluded due to either the absence of pain or low pain ratings [<10 on a numerical rating scale from 0 (no pain) to 100 (maximum tolerable pain)] during the familiarization run (n = 8), excessive startle responses in response to painful stimulation during the training run (n = 1), or technical issues with the response box used during catch trials (n = 1). The final sample comprised 48 participants (all right-handed, 23 females, age: 23.7 ± 3.4 y). Average clinical anxiety and depression scores obtained using the Hospital Anxiety and Depression Scale (75) were below clinically relevant cutoff scores of 8/21 (76) (anxiety: 3.0 ± 2.1; depression: 0.9 ± 1.1).

Procedure. To investigate how noxious stimulus intensity, expectations, and PEs relate to the cerebral processing of a painful stimulus and the preceding brain activity, the experiment incorporated two noxious heat stimulus intensities (hi and li) and two visual cues (HE and LE) resulting in four experimental conditions. HE cues were followed by hi stimuli in 75% of trials (hiHE) and li stimuli in 25% of trials (liHE). Conversely, LE cues were followed by li stimuli in 75% of trials (liLE) and by hi stimuli in 25% of trials (hiLE; Fig. 1A). The sequence of events for each trial is depicted in Fig. 1B. After a fixation period with a duration of 1.5 to 3 s, a visual cue (blue dot or yellow square) was presented for 1 s. At 1.5 s after the offset of the cue presentation, a brief painful heat stimulus was applied. At 3 s after the noxious stimulus, participants were prompted to rate the perceived pain intensity of the preceding painful heat stimulus on a numerical rating scale ranging from 0 (no pain) to 100 (maximum tolerable pain); a rating of 1 on this scale thus already indicates a minimally painful percept. To ensure sustained attention to the visual cues, a match-to-sample task was incorporated in 10% of the trials. In these catch trials, HE and LE cues were shown simultaneously after the pain rating and participants were asked to identify the cue of the current trial by a button press

Nickel et al.
Temporal–spectral signaling of sensory information and expectations in the cerebral processing of pain

PNAS | 7 of 10
https://doi.org/10.1073/pnas.2116616119

(left versus right, according to the position of the cue on the screen). Participants successfully focused on the task during the whole experiment as indicated by an average accuracy of 95.6 ± 0.1% during the match-to-sample task in catch trials. Trials were separated by 3 s, during which a white fixation cross was presented. The experiment consisted of four runs with 40 trials each (hiHE [$n = 15$], hiLE [$n = 5$], liLE [$n = 15$], liHE [$n = 5$]), resulting in total trial numbers of hiHE [$n = 60$], hiLE [$n = 20$], liLE [$n = 60$], liHE [$n = 20$]. Runs were separated by short breaks of ∼3 min. Contingencies between cues and stimulus intensities (i.e., whether a blue dot or a yellow square predicted hi/li stimuli and whether the blue dot/yellow square was presented either on the left or right side of the catch trial screen) were balanced across participants.

Prior to the main experiment, we applied a sequence of 10 heat stimuli with different intensities to familiarize the participants with the painful stimulation and the intensity rating procedure. Furthermore, participants were explicitly informed about the contingencies between cues and stimulus intensities and participated in a training run with 16 trials using the same experimental setup and contingencies as in the main experiment. The information and the training run were designed to ascertain that all participants were aware of the contingencies and to minimize learning during the main experiment. During the experiment, participants were seated in a comfortable chair and wore protective goggles and headphones playing white noise to cancel out ambient sounds.

Stimulation. Painful stimuli were applied to the dorsum of the left hand using a neodymium yttrium aluminum perovskite laser (Nd:YAP, Stimul 1340, DEKA M.E.L.A. srl) with a wavelength of 1,340 nm, a pulse duration of 4 ms, and a spot diameter of ∼7 mm (19). Stimulus intensity was set to 3.5 J for hi stimuli and 3 J for li stimuli (19). To avoid tissue damage and habituation/sensitization, the stimulation site was slightly changed after each stimulus.

Recordings and Preprocessing. EEG data were recorded using actiCAP snap/ slim with 64 active sensors (Easycap) placed according to the extended 10-20 system and BrainAmp MR plus amplifiers (Brain Products). All sensors were referenced to FCz and grounded at Fpz. The EEG was sampled at 1,000 Hz (0.1-μV resolution) and band-pass filtered between 0.016 and 250 Hz. Impedances were kept below 20 kΩ.

Preprocessing was performed using BrainVision Analyzer software (version 2.1.1.327, Brain Products). EEG data were downsampled to 500 Hz after low-pass filtering with a cutoff frequency of 225 Hz. To detect artifacts and to compute independent component (IC) weights, a 1-Hz high-pass filter (fourth-order Butterworth) and a 50-Hz notch filter removing line noise were applied. EEG data of all runs were concatenated. IC analysis based on the extended infomax algorithm was applied to the filtered EEG data ranging from −4.2 to 3.2 s with respect to laser stimulus onset and resulted in 64 ICs. ICs representing eye movements and muscle artifacts were identified (77). Subsequently, the identified ICs were subtracted from the unfiltered EEG, and data segments of 400 ms centered around data samples with amplitudes exceeding ±100 μV and data jumps exceeding 30 μV were automatically marked for rejection. Remaining artifacts were identified by visual inspection and manually marked for rejection. All electrodes were rereferenced to the average reference. Finally, data were exported to Matlab (version R2019b, Mathworks), and further analyses were performed using FieldTrip [version 20200128 (78)]. We segmented the EEG data into 7-s epochs ranging from −4 to 3 s with respect to the laser stimulus onset. All epochs including marked artifacts or trials in which the laser stimulus was not perceived as painful (pain rating = 0) were excluded from further analysis. To match the number of trials between both hi and both li conditions, respectively, the condition with the lowest trial count was identified for every participant, and the same number of trials was randomly drawn from the other conditions (maximum number = 20 trials). Further analyses were based on 17.7 ± 1.6 (range: 14 to 20) trials for hiHE/hiLE conditions and 15.3 ± 4.4 (range: 4 to 20) trials for liHE/liLE conditions for each participant.

Skin conductance data were recorded using two Ag/AgCl electrodes attached to the palmar distal phalanges of the left index and middle finger. Data were recorded using the GSR-MR module with constant voltage of 0.5 V and a BrainAmp ExG MR amplifier (Brain Products) with low-pass filtering at 250 Hz and a sampling frequency of 1,000 Hz. Subsequent offline analysis included low-pass filtering at 1 Hz using a fourth-order Butterworth filter, downsampling to 500 Hz, and a visual artifact inspection. Finally, data were exported and segmented into 14-s epochs ranging from −4 to 10 s with respect to the laser stimulus. Identical epochs as for the EEG analyses were selected. Furthermore, we had to exclude additional epochs of skin conductance data comprising marked artifacts. As a result, further analyses of skin conductance data were based on 17.7 ± 1.8 (range: 14 to 20) and 17.6 ± 1.6 (range: 14 to 20) trials for hiHE and hiLE conditions, respectively, and 15.2 ±

4.7 (range: 4 to 20) and 15.2 ± 4.8 (range: 4 to 20) trials for liHE and liLE conditions, respectively.

Time-Domain Analysis of EEG Data. To quantify the amplitudes of laser-evoked N1, N2, and P2 responses, EEG data were band-pass filtered between 1 and 30 Hz (fourth-order Butterworth), and a baseline correction was applied using the time interval −3.3 and −2.8 s before the painful stimulus. The selected baseline interval preceded the visual cue to avoid expectation effects during the baseline period. To investigate the amplitude of the N1, the data were rereferenced to Fz. First, the latencies of all laser-evoked responses were assessed for each participant using the average across all trials and conditions. We used a peak/trough detection procedure within the time windows 120 to 20, 180 to 30, and 250 to 500 ms (19) for the N1, N2, and P2, respectively. Second, to obtain the amplitudes of the average evoked responses, trials were averaged separately for each condition. Amplitudes of N1, N2, and P2 were assessed by averaging a 30-ms window centered at respective latencies determined in the previous step. Amplitudes of N1 and N2/P2 were extracted at channel C4 (79) and Cz, respectively. Finally, single-trial estimates of N1, N2, and P2 amplitudes were obtained accordingly by averaging single-trial data across the same 30-ms windows centered at the latencies identified in step one. For the N1, three participants were excluded from statistical analyses due to a lack of a response in step one.

Besides laser-evoked poststimulus responses, we were interested in prestimulus differences in brain activity induced by the expectation of high or low stimuli. Hence, we investigated the SPN by averaging the amplitude at Cz across the 500-ms interval directly preceding the laser stimulus (29). All HE and LE trials were averaged separately for each participant. A low-pass filter with a cutoff frequency of 30 Hz (fourth-order Butterworth) and a baseline correction using the time interval between −3.3 and −2.8 s were applied. No further high-pass filter was applied to take low frequencies of the SPN into account. As a consequence, five participants had to be excluded from this analysis due to sweating artifacts, which could be corrected by high-pass filtering when laser-evoked responses were analyzed.

Time–Frequency Analysis of EEG Data. To quantify the power of laser-induced oscillatory responses, data were transformed to the time–frequency domain. To this end, we applied a fourth-order Butterworth high-pass filter of 1 Hz and a band-stop filter of 49 to 51 Hz to dampen line noise. Subsequently, a fast Fourier transformation was applied to Hanning-tapered EEG data with a moving time window of 500-ms length for the frequencies from 1 to 30 Hz and a window of 250-ms length for the frequencies from 31 to 100 Hz. The step size was set to 20 ms. We chose a longer window for lower frequencies to retrieve more accurate power estimates, including at least four cycles for frequencies above 8 Hz. To obtain average responses at different frequency bands, time–frequency data were averaged across trials separately for each of the four conditions. Responses at alpha (8 to 12 Hz), beta [13 to 30 Hz (72)], and gamma [70 to 90 Hz (80)] frequency bands were quantified using the time windows 500 to 900, 300 to 600 (81, 82), and 150 to 350 ms (80), respectively. Alpha and beta power was estimated at sensors Cz, C2, C4, CPz, CP2, and CP4 covering the somatosensory cortex (19, 81, 82). Gamma power was retrieved at sensor Cz (19). Average responses at the different frequency bands were assessed by calculating the mean power estimates across the selected frequencies, time windows, and channels (region of interest, ROI). Consequently, we obtained three power values for each condition (i.e., 12 power values for each participant). Single-trial responses of different frequency bands were quantified by averaging across the same time–frequency sensor selection as for the average responses for each trial. All power values were not baseline corrected (see *SI Appendix*, Table S1 for results with baseline correction using the interval −750 to −250 ms preceding the laser stimulus as baseline).

In addition to oscillatory poststimulus responses, we were interested in prestimulus differences in oscillatory brain activity induced by the expectation of hi or li stimuli. Prestimulus alpha (8 to 12 Hz) and beta (13 to 30 Hz) power were obtained using the mean power across the time windows −2.5 to −1.5 s as well as −1.25 to −0.25 s and the sensors Cz, C2, C4, CPz, CP2, and CP4. We chose these time windows to investigate power differences during cue presentation (−2.5 to −1.5 s) and closely before laser stimulus onset (−1.25 to −0.25 s). Data immediately preceding the laser stimulus were not analyzed to avoid confounding prestimulus power estimates with poststimulus activity due to the 500-ms sliding window.

Analysis of Skin Conductance Data. To quantify SCRs, epochs of skin conductance data were averaged across trials for each condition and participant. Amplitudes were defined as peak amplitudes of the maximal peak within a time window from 1 to 7.8 s poststimulus following a peak detection

procedure (79, 82) and a baseline correction using skin conductance data at time point zero of the laser stimulus onset. Prior to the quantification of SCRs, we identified nonresponders by averaging skin conductance data across all trials and conditions for each participant. If the detected global amplitude was below 0.05 μS, participants were defined as nonresponders (83). Based on these criteria, 17 participants were classified as nonresponders and excluded from further analysis of SCR data.

Statistical Analyses. Statistical analyses were performed using the statistical software packages JASP [version 0.14.1 (84)] and R [version 3.6 (85)]. Motivated by previous findings (50, 53), we investigated five different response patterns (Fig. 2), which vary with respect to the integrated predictors. Specifically, the predictors stimulus intensity (INT), expectation (EXP), PE, a linear combination of stimulus intensity and expectation (EXP+INT) as well as a linear combination of expectation and PE (EXP+PE) were investigated. The latter has been termed the predictive coding model (43). To investigate these patterns, we computed rmANOVAs for each poststimulus response (pain rating, N1, N2, P2, alpha, beta and gamma-power, and SCR) as dependent variable using stimulus intensity (hi versus li) and cue (HE versus LE) as factors. Bayesian rmANOVAs were performed as these allow to specifically provide evidence for the null hypothesis of no effect (54). In Bayesian rmANOVAs, the BF is defined as ratio between the likelihood of the data given a model including the effect of interest and the likelihood of the data given an equivalent model with the effect of interest removed. BF < 0.33 and BF < 0.10 indicate moderate and strong evidence in favor of the absence of the effect of interest, respectively. BF > 3 and BF > 10 indicate moderate and strong evidence in favor of the effect of interest, respectively (54). For all Bayesian statistics, default Cauchy priors were chosen in JASP. Complementing Bayesian inference, we also conducted frequentist rmANOVAs with the same factors. Post hoc dependent samples Student's *t* tests were performed if a statistically significant interaction was observed. To test for additional effects outside the predefined ROIs, we performed cluster-based permutation tests across time, frequencies, and all channels (see *SI Appendix* for details).

Furthermore, on a single-trial level, we performed formal pairwise model comparisons to test which model explains poststimulus responses best. Models including stimulus intensity and expectation (INT+EXP) as well as expectation and PE (EXP+PE) as predictors were compared to the model solely including stimulus intensity (INT), respectively. Additionally, the EXP+PE model was compared with the INT+EXP model. Linear mixed effects models included either stimulus intensity, expectation, PE, or combinations thereof as fixed effects and participants as random effects. In contrast to the rmANOVA approach, linear mixed effects models are based on single-trial data and account for differences in trial numbers and variability between subjects. Moreover, the different models can be explicitly formulated and compared.

We used the R package BayesFactor [version 0.9.12 (86)] to compute BFs for model comparisons. These BFs quantify the evidence for one model over another model as a ratio of two likelihoods (i.e., the likelihood of the data given each model). Stimulus intensity was coded as 1 for hi stimuli and as 0 for li stimuli. Expectation was coded as the probability of a following hi stimulus [i.e., 0.75 for hi cue conditions (hiHE and liHE) and 0.25 for li cue conditions (hiLE and liLE)]. Finally, the PE was defined as aversive PE, meaning that a PE occurs only if the outcome (stimulus intensity) is more painful than expected. Specifically, the aversive PE was selected because a previous study by Geuter, Boll, Eippert, and Buchel (50) demonstrated that models incorporating the aversive PE explained brain responses to pain better than absolute and signed PEs. Hence, it was coded as difference between stimulus intensity and expectation [i.e., PE = 1 to 0.25 for hiLE, PE = 1 to 0.75 for hiHE, and PE = 0 for for liHE and liLE (50); see *SI Appendix*, Fig. S2 for Bayesian model comparisons using additional absolute and signed PE formulations].

To complement univariate analyses using single poststimulus responses as outcome variables and to investigate whether a combination of N1, N2, P2, alpha, beta, and gamma power can predict the expectation effect on pain ratings, we computed difference values of pain ratings, N1, N2, P2, alpha, beta, and gamma power by subtracting average values of the LE trials from HE trials for each participant. Subsequently, we tried to predict difference values of pain ratings (dependent variable) based on difference values of N1, N2, P2, alpha, beta, and gamma power (independent variables) using multiple regression. Prior to the analysis, all difference values were z-transformed across participants to adjust the data to the same scale.

Finally, we investigated whether cue-induced expectations affected brain activity preceding the laser stimulus. To this end, we performed Bayesian-dependent samples Student's *t* tests comparing the average amplitude of the SPN between HE and LE trials. Similarly, we compared alpha and beta power during two prestimulus windows, one during cue presentation and one closely preceding the painful laser stimulus. Again, these tests were accompanied by Bayesian-dependent samples *t* tests to estimate the evidence for the null hypothesis. To test for additional effects outside the predefined ROIs, we performed cluster-based permutation tests across time, frequencies, and all channels (see *SI Appendix* for details).

1. L. Y. Atlas, T. D. Wager, How expectations shape pain. *Neurosci. Lett.* **520**, 140–148 (2012).
2. H. L. Fields, How expectations influence pain. *Pain* **159** (suppl. 1), S3–S10 (2018).
3. K. J. Peerdeman, A. I. van Laarhoven, M. L. Peters, A. W. Evers, An integrative review of the influence of expectancies on pain. *Front. Psychol.* **7**, 1270 (2016).
4. D. G. Finniss, T. J. Kaptchuk, F. Miller, F. Benedetti, Biological, clinical, and ethical advances of placebo effects. *Lancet* **375**, 686–695 (2010).
5. P. Enck, U. Bingel, M. Schedlowski, W. Rief, The placebo response in medicine: Minimize, maximize or personalize? *Nat. Rev. Drug Discov.* **12**, 191–204 (2013).
6. T. D. Wager, L. Y. Atlas, The neuroscience of placebo effects: Connecting context, learning and health. *Nat. Rev. Neurosci.* **16**, 403–418 (2015).
7. J. W. S. Vlaeyen, G. Crombez, S. J. Linton, The fear-avoidance model of pain. *Pain* **157**, 1588–1589 (2016).
8. S. Cormier, G. L. Lavigne, M. Choinière, P. Rainville, Expectations predict chronic pain treatment outcomes. *Pain* **157**, 329–338 (2016).
9. K. J. Peerdeman et al., Relieving patients' pain with expectation interventions: A meta-analysis. *Pain* **157**, 1179–1191 (2016).
10. M. N. Baliki, A. V. Apkarian, Nociception, pain, negative moods, and behavior selection. *Neuron* **87**, 474–491 (2015).
11. L. Garcia-Larrea, R. Peyron, Pain matrices and neuropathic pain matrices: A review. *Pain* **154** (suppl. 1), S29–S43 (2013).
12. M. Ploner, E. S. May, Electroencephalography and magnetoencephalography in pain research-current state and future perspectives. *Pain* **159**, 206–211 (2018).
13. L. Garcia-Larrea, M. Frot, M. Valeriani, Brain generators of laser-evoked potentials: From dipoles to functional significance. *Neurophysiol. Clin.* **33**, 279–292 (2003).
14. J. Lorenz, L. Garcia-Larrea, Contribution of attentional and cognitive factors to laser evoked brain potentials. *Neurophysiol. Clin.* **33**, 293–301 (2003).
15. M. Ploner, C. Sorg, J. Gross, Brain rhythms of pain. *Trends Cogn. Sci.* **21**, 100–110 (2017).
16. L. García-Larrea, R. Peyron, B. Laurent, F. Mauguière, Association and dissociation between laser-evoked potentials and pain perception. *Neuroreport* **8**, 3785–3789 (1997).
17. M. C. Lee, A. Mouraux, G. D. Iannetti, Characterizing the cortical activity through which pain emerges from nociception. *J. Neurosci.* **29**, 7909–7916 (2009).
18. J. Gross, A. Schnitzler, L. Timmermann, M. Ploner, Gamma oscillations in human primary somatosensory cortex reflect pain perception. *PLoS Biol.* **5**, e133 (2007).
19. L. Hu, G. D. Iannetti, Neural indicators of perceptual variability of pain across species. *Proc. Natl. Acad. Sci. U.S.A.* **116**, 1782–1791 (2019).
20. T. D. Wager, D. Matre, K. L. Casey, Placebo effects in laser-evoked pain potentials. *Brain Behav. Immun.* **20**, 219–230 (2006).
21. L. Colloca et al., Learning potentiates neurophysiological and behavioral placebo analgesic responses. *Pain* **139**, 306–314 (2008).
22. L. Tiemann et al., Differential neurophysiological correlates of bottom-up and top-down modulations of pain. *Pain* **156**, 289–296 (2015).
23. P. S. Lyby, P. M. Aslaksen, M. A. Flaten, Variability in placebo analgesia and the role of fear of pain—An ERP study. *Pain* **152**, 2405–2412 (2011).
24. D. L. Morton, W. El-Deredy, A. Watson, A. K. Jones, Placebo analgesia as a case of a cognitive style driven by prior expectation. *Brain Res.* **1359**, 137–141 (2010).
25. E. J. Hird, A. K. P. Jones, D. Talmi, W. El-Deredy, A comparison between the neural correlates of laser and electric pain stimulation and their modulation by expectation. *J. Neurosci. Methods* **293**, 117–127 (2018).
26. G. D. Iannetti, N. P. Hughes, M. C. Lee, A. Mouraux, Determinants of laser-evoked EEG responses: Pain perception or stimulus saliency? *J. Neurophysiol.* **100**, 815–828 (2008).
27. N. T. Huneke et al., Experimental placebo analgesia changes resting-state alpha oscillations. *PLoS One* **8**, e78278 (2013).
28. J. Lorenz et al., Cortical correlates of false expectations during pain intensity judgments—A possible manifestation of placebo/nocebo cognitions. *Brain Behav. Immun.* **19**, 283–295 (2005).
29. C. A. Brown, B. Seymour, Y. Boyle, W. El-Deredy, A. K. P. Jones, Modulation of pain ratings by expectation and uncertainty: Behavioral characteristics and anticipatory neural correlates. *Pain* **135**, 240–250 (2008).
30. Y. Huang, R. P. N. Rao, Predictive coding. *Wiley Interdiscip. Rev. Cogn. Sci.* **2**, 580–593 (2011).

Nickel et al.
Temporal–spectral signaling of sensory information and expectations in the cerebral processing of pain

PNAS | 9 of 10
https://doi.org/10.1073/pnas.2116616119

NEUROSCIENCE

31. A. Clark, Whatever next? Predictive brains, situated agents, and the future of cognitive science. *Behav. Brain Sci.* **36**, 181–204 (2013).

32. F. P. de Lange, M. Heilbron, P. Kok, How do expectations shape perception? *Trends Cogn. Sci.* **22**, 764–779 (2018).

33. K. Friston, The free-energy principle: A unified brain theory? *Nat. Rev. Neurosci.* **11**, 127–138 (2010).

34. K. Friston, A theory of cortical responses. *Philos. Trans. R. Soc. Lond. B Biol. Sci.* **360**, 815–836 (2005).

35. L. H. Arnal, A. L. Giraud, Cortical oscillations and sensory predictions. *Trends Cogn. Sci.* **16**, 390–398 (2012).

36. A. M. Bastos et al., Canonical microcircuits for predictive coding. *Neuron* **76**, 695–711 (2012).

37. A. Bendixen, I. SanMiguel, E. Schröger, Early electrophysiological indicators for predictive processing in audition: A review. *Int. J. Psychophysiol.* **83**, 120–131 (2012).

38. K. Rauss, S. Schwartz, G. Pourtois, Top-down effects on early visual processing in humans: A predictive coding framework. *Neurosci. Biobehav. Rev.* **35**, 1237–1253 (2011).

39. G. Stefanics, J. Heinzle, A. A. Horváth, K. E. Stephan, Visual mismatch and predictive coding: A computational single-trial ERP study. *J. Neurosci.* **38**, 4020–4030 (2018).

40. W. Sedley et al., Neural signatures of perceptual inference. *eLife* **5**, e11476 (2016).

41. A. M. Bastos et al., Visual areas exert feedforward and feedback influences through distinct frequency channels. *Neuron* **85**, 390–401 (2015).

42. G. Michalareas et al., Alpha-beta and gamma rhythms subserve feedback and feedforward influences among human visual cortical areas. *Neuron* **89**, 384–397 (2016).

43. C. Büchel, S. Geuter, C. Sprenger, F. Eippert, Placebo analgesia: A predictive coding perspective. *Neuron* **81**, 1223–1239 (2014).

44. A. Tabor, M. A. Thacker, G. L. Moseley, K. P. Körding, Pain: A statistical account. *PLOS Comput. Biol.* **13**, e1005142 (2017).

45. G. Ongaro, T. J. Kaptchuk, Symptom perception, placebo effects, and the Bayesian brain. *Pain* **160**, 1–4 (2019).

46. B. Seymour, Pain: A precision signal for reinforcement learning and control. *Neuron* **101**, 1029–1041 (2019).

47. M. J. Edwards, R. A. Adams, H. Brown, I. Pareés, K. J. Friston, A Bayesian account of 'hysteria'. *Brain* **135**, 3495–3512 (2012).

48. P. Henningsen et al., EURONET-SOMA Group, Persistent physical symptoms as perceptual dysregulation: A neuropsychobehaviral model and its clinical implications. *Psychosom. Med.* **80**, 422–431 (2018).

49. K. Wiech, Deconstructing the sensation of pain: The influence of cognitive processes on pain perception. *Science* **354**, 584–587 (2016).

50. S. Geuter, S. Boll, F. Eippert, C. Büchel, Functional dissociation of stimulus intensity encoding and predictive coding of pain in the insula. *eLife* **6**, e24770 (2017).

51. S. Fazeli, C. Büchel, Pain-related expectation and prediction error signals in the anterior insula are not related to aversiveness. *J. Neurosci.* **38**, 6461–6474 (2018).

52. A. Strube, M. Rose, S. Fazeli, C. Büchel, The temporal and spectral characteristics of expectations and prediction errors in pain and thermoception. *eLife* **10**, e62809 (2021).

53. T. Egner, J. M. Monti, C. Summerfield, Expectation and surprise determine neural population responses in the ventral visual stream. *J. Neurosci.* **30**, 16601–16608 (2010).

54. C. Keysers, V. Gazzola, E. J. Wagenmakers, Using Bayes factor hypothesis testing in neuroscience to establish evidence of absence. *Nat. Neurosci.* **23**, 788–799 (2020).

55. M. Allen, D. Poggiali, K. Whitaker, T. R. Marshall, R. A. Kievit, Raincloud plots: A multi-platform tool for robust data visualization. *Wellcome Open Res.* **4**, 63 (2019).

56. K. S. Button et al., Power failure: Why small sample size undermines the reliability of neuroscience. *Nat. Rev. Neurosci.* **14**, 365–376 (2013).

57. J. P. Ioannidis, M. R. Munafò, P. Fusar-Poli, B. A. Nosek, S. P. David, Publication and other reporting biases in cognitive sciences: Detection, prevalence, and prevention. *Trends Cogn. Sci.* **18**, 235–241 (2014).

58. L. Plaghki, A. Mouraux, How do we selectively activate skin nociceptors with a high power infrared laser? Physiology and biophysics of laser stimulation. *Neurophysiol. Clin.* **33**, 269–277 (2003).

59. A. Todorovic, F. P. de Lange, Repetition suppression and expectation suppression are dissociable in time in early auditory evoked fields. *J. Neurosci.* **32**, 13389–13395 (2012).

60. A. Todorovic, F. van Ede, E. Maris, F. P. de Lange, Prior expectation mediates neural adaptation to repeated sounds in the auditory cortex: An MEG study. *J. Neurosci.* **31**, 9118–9123 (2011).

61. Y. Song et al., Predictive coding models for pain perception. *J. Comput. Neurosci.* **49**, 107–127 (2021).

62. V. Legrain, G. D. Iannetti, L. Plaghki, A. Mouraux, The pain matrix reloaded: A salience detection system for the body. *Prog. Neurobiol.* **93**, 111–124 (2011).

63. K. D. Davis et al., Discovery and validation of biomarkers to aid the development of safe and effective pain therapeutics: Challenges and opportunities. *Nat. Rev. Neurol.* **16**, 381–400 (2020).

64. Y. Tu, Y. Bi, L. Zhang, H. Wei, L. Hu, Mesocorticolimbic pathways encode cue-based expectancy effects on pain. *J. Neurosci.* **40**, 382–394 (2020).

65. L. A. Henderson et al., Effect of expectation on pain processing: A psychophysics and functional MRI analysis. *Front. Neurosci.* **14**, 6 (2020).

66. Y. W. Shih et al., Effects of positive and negative expectations on human pain perception engage separate but interrelated and dependently regulated cerebral mechanisms. *J. Neurosci.* **39**, 1261–1274 (2019).

67. A. Grahl, S. Onat, C. Büchel, The periaqueductal gray and Bayesian integration in placebo analgesia. *eLife* **7**, e32930 (2018).

68. M. Zunhammer, U. Bingel, T. D. Wager, C. Placebo Imaging; Placebo Imaging Consortium, Placebo effects on the neurologic pain signature: A meta-analysis of individual participant functional magnetic resonance imaging data. *JAMA Neurol.* **75**, 1321–1330 (2018).

69. C. W. Woo et al., Quantifying cerebral contributions to pain beyond nociception. *Nat. Commun.* **8**, 14211 (2017).

70. C. W. Woo, M. Roy, J. T. Buhle, T. D. Wager, Distinct brain systems mediate the effects of nociceptive input and self-regulation on pain. *PLoS Biol.* **13**, e1002036 (2015).

71. L. Koban, M. Jepma, M. López-Solà, T. D. Wager, Different brain networks mediate the effects of social and conditioned expectations on pain. *Nat. Commun.* **10**, 4096 (2019).

72. C. Pernet et al., Issues and recommendations from the OHBM COBIDAS MEEG committee for reproducible EEG and MEG research. *Nat. Neurosci.* **23**, 1473–1483 (2020).

73. F. Faul, E. Erdfelder, A. G. Lang, A. Buchner, G*Power 3: A flexible statistical power analysis program for the social, behavioral, and biomedical sciences. *Behav. Res. Methods* **39**, 175–191 (2007).

74. J. Correll, C. Mellinger, G. H. McClelland, C. M. Judd, Avoid Cohen's 'Small', 'Medium', and 'Large' for power analysis. *Trends Cogn. Sci.* **24**, 200–207 (2020).

75. A. S. Zigmond, R. P. Snaith, The hospital anxiety and depression scale. *Acta Psychiatr. Scand.* **67**, 361–370 (1983).

76. I. Bjelland, A. A. Dahl, T. T. Haug, D. Neckelmann, The validity of the Hospital Anxiety and Depression Scale. An updated literature review. *J. Psychosom. Res.* **52**, 69–77 (2002).

77. T. P. Jung et al., Removing electroencephalographic artifacts by blind source separation. *Psychophysiology* **37**, 163–178 (2000).

78. R. Oostenveld, P. Fries, E. Maris, J.-M. Schoffelen, FieldTrip: Open source software for advanced analysis of MEG, EEG, and invasive electrophysiological data. *Comput. Intell. Neurosci.* **2011**, 156869 (2011).

79. L. Hu, A. Mouraux, Y. Hu, G. D. Iannetti, A novel approach for enhancing the signal-to-noise ratio and detecting automatically event-related potentials (ERPs) in single trials. *Neuroimage* **50**, 99–111 (2010).

80. L. Tiemann et al., Distinct patterns of brain activity mediate perceptual and motor and autonomic responses to noxious stimuli. *Nat. Commun.* **9**, 4487 (2018).

81. A. Mouraux, J. M. Guerit, L. Plaghki, Non-phase locked electroencephalogram (EEG) responses to CO_2 laser skin stimulations may reflect central interactions between A-delta- and C-fibre afferent volleys. *Clin. Neurophysiol.* **114**, 710–722 (2003).

82. M. Ploner, J. Gross, L. Timmermann, B. Pollok, A. Schnitzler, Pain suppresses spontaneous brain rhythms. *Cereb. Cortex* **16**, 537–540 (2006).

83. W. Boucsein, *Electrodermal Activity* (Springer, New York, 2012).

84. JASP Team, JASP (Version 0.14.1) (Computer software) (2020).

85. R Core Team, *R: A Language and Environment for Statistical Computing* (R Foundation for Statistical Computing, Vienna, Austria, 2021).

86. J. N. Rouder, R. D. Morey, Default Bayes factors for model selection in regression. *Multivariate Behav. Res.* **47**, 877–903 (2012).

87. C. R. Pernet et al., EEG-BIDS, an extension to the brain imaging data structure for electroencephalography. *Sci. Data* **6**, 103 (2019).

10 of 10 | PNAS

https://doi.org/10.1073/pnas.2116616119

Nickel et al.
Temporal–spectral signaling of sensory information and expectations in the cerebral processing of pain